

Anisotropic dynamical spin-density response in quantum wells with spin-orbit interaction

Priscilla E. Iglesias and Jesús A. Maytorena

Centro de Nanociencias y Nanotecnología, Universidad Nacional Autónoma de México, Apdo. Postal 2681, Ensenada, 22800 Baja California, México

(Received 1 September 2010; published 19 November 2010)

The electric field-induced spin polarization of a two-dimensional electron gas with spin-orbit interaction is investigated in the frequency domain. We calculate the spin-polarizability tensor using the linear-response theory, taking into account the presence of both Rashba and Dresselhaus spin-orbit couplings. We consider quantum wells grown in the main crystallographic directions and concentrate on the high-frequency response in the collisionless regime. For an anisotropic spin splitting, it is shown that the spin-density response becomes dependent on the direction of the applied electric field and presents characteristic spectral features, in notable contrast to the case of an isotropic spin-orbit coupling. Such behavior is explained in terms of the nonisotropic momentum space available for electric-dipole transitions and the presence of critical points. This anisotropic dynamic response suggests new possibilities of spin manipulation which could find spintronic applications.

DOI: [10.1103/PhysRevB.82.205324](https://doi.org/10.1103/PhysRevB.82.205324)

PACS number(s): 72.25.Dc

I. INTRODUCTION

The generation of spin currents and spin densities in semiconductor structures as a response to external electric fields is a major issue under intense experimental and theoretical study.¹⁻⁴ The coupling between the spin of electrons and electric fields via spin-orbit interaction (SOI) is the central mechanism behind many concepts and ideas in semiconductor spintronics.^{5,6} The tunability of this interaction in systems with reduced symmetry through electrical gating has motivated the search for new ways of manipulating electron spins without employing magnetic materials and external magnetic fields.⁷ Among the mechanisms of spin-density generation, the magnetoelectric effect called electric field-induced or current-induced spin polarization (CISP) is one of the most important. It has been observed in SO-coupled systems like two-dimensional electron gases (2DEG) or quantum wells (QWs) formed in semiconductor heterostructures.⁸⁻¹² In this class of systems the dominant SO contributions are the Rashba (R) and Dresselhaus (D) couplings. Several interesting spin-related effects and devices relying on the interplay of these SO mechanisms have been predicted and proposed recently. A nonballistic version of the Datta-Das spin transistor,¹³ the absence of spin polarization for finite frequencies at equal SO strengths,^{14,15} and the existence of a persistent spin helix^{16,17} are some relevant examples requiring the simultaneous presence of the Rashba and Dresselhaus SOI. Further examples include electrically induced spin accumulation in diffusive finite-sized systems,¹⁸ the dc generation of an anisotropic CISP,¹⁹ SOI-induced anisotropies of plasmon dynamics,²⁰ or the static spin response of quantum wells grown along different directions,²¹ all of which are based on the anisotropic spin-splitting characteristic of the combined SO mechanisms.

The spin splitting caused by SOI in quasi-two-dimensional electron systems opens the possibility of resonant effects involving electric-dipole transitions between the spin-split subbands as a response to alternating electric fields at frequency in the terahertz regime.^{22,23} The importance of considering the dynamical regime (frequency-dependent re-

sponse) in the presence of R+D SOI has been emphasized in several studies.^{14,15,24} Charge optical conductivities²⁵ and spin susceptibilities,^{26,27} plasmon modes,²⁰ spin-current injection in quantum wells by optical absorption,²⁸ and spin density induced by electromagnetic waves,²⁹ among others related physical problems have been investigated.

The frequency dependence of CISP due to an ac electric field in a R+D SO-coupled system has been addressed in Refs. 14 and 15. In the former study, the discussion was focused mainly on the behavior of the spin polarizability tensor at low frequencies as a function of the SO-coupling strengths, in quantum wells grown in [001] and [110] crystallographic directions. The latter authors discuss the identification of the resonances in the spin response of a [001]-grown quantum well by tuning the strength of the Rashba and Dresselhaus couplings or the excitation frequency, considering only two particular directions of the applied electric field. Trushin and Schliemann¹⁹ also studied CISP in [001] quantum well with R+D SOI but excited by a dc external field and also noted the dependence of the spin accumulation on the direction of the field.

Following these studies, in the present paper we further investigate CISP in a 2DEG with R+D SOI as generated by a frequency-dependent, spatially homogeneous, in-plane electric field. We consider Hamiltonians corresponding to samples grown in the [001], [110], and [111] directions and calculate the spin-polarizability tensor and the magnitude of the spin-polarization density as a function of the exciting frequency and of the angle specifying the direction of the electric field vector. We assume that the frequency exceeds relaxation and scattering rates and, for simplicity, ignore the static limit in our calculations. It is known that in full diagrammatic calculations the corrections to the intrinsic spin response vanish for increasing frequencies and low-impurity densities.^{6,14,30} Thus, we concentrate on the high-frequency response in the clean regime (weak disorder or strong SOI) and explain the structure of the calculated spectra in terms of the anisotropic momentum space available for optical transitions. In contrast to Refs. 14 and 15 we focus on the *magnitude* of the frequency-dependent spin polarization in addition to the polarizability response functions. We found that the

overall aspect of the spin polarization with respect to the mentioned electric field angle follows the same functional angular dependence as that of the function giving the spin-splitting energy. This adds a new element of control of the spin response of this type of systems, which is an aspect not sufficiently explored.

II. MODEL

We consider a 2D electron gas lying at $z=0$ plane with one-electron Hamiltonian $H = \frac{\hbar^2 k^2}{2m} + H_{\text{SO}}$, where the spin-orbit interaction is written as

$$H_{\text{SO}} = \frac{\hbar}{2} \Omega_i \sigma_i = \sigma_i \mu_{ij} k_j \quad (i, j = x, y, z). \quad (1)$$

Here we adopt the convention of sum over any repeated index, m is the effective mass, σ_i are the Pauli matrices, and $(\hbar/2)\mathbf{\Omega}(\mathbf{k})$ is the effective spin-orbit field, which we assume linear in the electron wave vector $\mathbf{k} = (k_x, k_y, 0)$. The matrix $\mu_{ij} = (\hbar/2) \partial \Omega_i / \partial k_j$ contains the parameters characterizing the strengths of SO couplings due to structural inversion asymmetry (Rashba coupling) and bulk inversion asymmetry (Dresselhaus coupling). For narrow QWs grown along the [001], [110], and [111] directions this matrix takes the form

$$\mu_{ij} = \begin{pmatrix} -\beta_{[001]} & \alpha & 0 \\ -\alpha & \beta_{[001]} & 0 \\ 0 & 0 & 0 \end{pmatrix} \quad \mu_{ij} = \begin{pmatrix} 0 & \alpha & 0 \\ -\alpha & 0 & 0 \\ \beta_{[110]} & 0 & 0 \end{pmatrix}$$

$$\mu_{ij} = \begin{pmatrix} 0 & \tilde{\alpha} & 0 \\ -\tilde{\alpha} & 0 & 0 \\ 0 & 0 & 0 \end{pmatrix},$$

respectively, where α is the SO-coupling strength of the Rashba interaction, $\beta_{[hkl]}$ is the SO parameter of the Dresselhaus coupling of a sample grown in the crystallographic direction $[hkl]$, and $\tilde{\alpha} = \alpha + \beta_{[111]}$. For a [001]-grown QW, the coordinate system x, y, z is $x \parallel [100]$, $y \parallel [010]$, $z \parallel [001]$; for a [110]-grown QW, $z \parallel [110]$, $x \parallel [\bar{1}10]$, $y \parallel \mathbf{z} \times x \parallel [001]$, and for a [111]-grown QW, $z \parallel [111]$, $y \parallel [\bar{1}10]$, $x \parallel \mathbf{y} \times \mathbf{z} \parallel [11\bar{2}]$.³¹ The energy spectrum of the above Hamiltonian is $\varepsilon_\lambda(\mathbf{k}) = \hbar k^2 / 2m + \lambda |\Delta(\mathbf{k})| / 2$, where $\lambda = \pm$ specifies the chirality of the spin states $|\mathbf{k}\lambda\rangle$ and the upper (+) and lower (-) parts of the spectrum. The quantity $\Delta(\mathbf{k}) = \hbar |\mathbf{\Omega}(\mathbf{k})|$ determines the energy spin splitting $\Delta(\mathbf{k}) \equiv \varepsilon_+(\mathbf{k}) - \varepsilon_-(\mathbf{k})$. Introducing polar coordinates for the in-plane motion $(k_x, k_y) = k(\cos \theta, \sin \theta)$, the energy of the spin-split subbands can be written as $\varepsilon_\lambda(k, \theta) = \hbar^2 \{ [k + \lambda \kappa_{\text{SO}}(\theta)]^2 - k_{\text{SO}}^2(\theta) \} / 2m$ in terms of a characteristic SO momentum $k_{\text{SO}}(\theta) = mg_{[hkl]}(\theta) / \hbar^2$, where the function $g_{[hkl]}(\theta) = \sqrt{\mu_{ij} \mu_{ij} \hat{k}_i \hat{k}_j}$, $\hat{k}_i(\theta) = k_i / k$, describes the anisotropy of the spin-splitting $\Delta(\mathbf{k}) = 2kg_{[hkl]}(\theta)$ for each growth direction $[hkl]$ of the sample. Explicitly,

$$g_{[001]}(\theta) = \sqrt{\alpha^2 + \beta_{[001]}^2 - 2\alpha\beta_{[001]} \sin 2\theta},$$

$$g_{[110]}(\theta) = \sqrt{\alpha^2 + \frac{1}{2}\beta_{[110]}^2 + \frac{1}{2}\beta_{[110]}^2 \cos 2\theta},$$

and $g_{[111]}(\theta) = \tilde{\alpha}$. In particular, for $[hkl] = [001]$ with only Rashba or Dresselhaus coupling, for $[hkl] = [110]$ with only Rashba coupling, and for $[hkl] = [111]$ with both types of coupling, the spin splitting is isotropic. At zero temperature and at the (positive) Fermi energy level ε_F , there are two different Fermi wave vectors $k_F^\lambda(\theta) = \sqrt{2m\varepsilon_F / \hbar^2 + k_{\text{SO}}^2(\theta)} - \lambda k_{\text{SO}}(\theta)$, determined from $\varepsilon_\lambda[k_F^\lambda(\theta), \theta] = \varepsilon_F$, where $\varepsilon_F = \hbar^2(k_0^2 - 2\kappa_{\text{SO}}^2) / 2m$ with $k_0 = \sqrt{2\pi n}$ being the Fermi wave vector of a spin-degenerate 2DEG with density n and $\kappa_{\text{SO}} = m\sqrt{\mu_{ij} \mu_{ij}} / 2 / \hbar^2$. We shall use the symbol R+D $[hkl]$ to denote each Hamiltonian case.

III. DYNAMICAL SPIN-POLARIZATION RESPONSE

Within the linear-response theory, the spin-polarization density $S_i = \hbar \langle \sigma_i \rangle / 2$ induced by an homogeneous in-plane electric field $\mathbf{E} = [E_x(\omega)\hat{\mathbf{x}} + E_y(\omega)\hat{\mathbf{y}}] e^{-i\omega t} e^{\eta t}$ is given by $\langle \sigma_i(\omega) \rangle = \gamma_{ij}(\omega) E_j(\omega)$. The response function γ_{ij} is determined from the Kubo formula

$$\gamma_{ij}(\omega) = \langle \langle \sigma_i; e v_j \rangle \rangle / \hbar \tilde{\omega}$$

with $\tilde{\omega} = \omega + i\eta$, where $\langle \langle A; B \rangle \rangle$ is a short notation for the Fourier transform $\int_0^\infty e^{i\tilde{\omega}t} \langle [A(t), B(0)] \rangle dt$ ($\eta \rightarrow 0^+$). The symbol $\langle \langle A(t), B(0) \rangle \rangle = \sum_\lambda \int d^2k f[\varepsilon_\lambda(\mathbf{k})] \langle \langle \mathbf{k}\lambda | [A(t), B(0)] | \mathbf{k}\lambda \rangle \rangle$ indicates quantum and thermal averaging of the commutator of the operators A and B and $f(\varepsilon)$ is the Fermi distribution function. The spin-polarizability γ_{ij} involves the velocity operator $v_i(\mathbf{k}) = (1/\hbar) \partial H / \partial k_i = \hbar k_i / m + \sigma_i \mu_{il} / \hbar$, and it can be expressed as the linear combination

$$\gamma_{ij}(\omega) = \frac{e}{i\hbar \tilde{\omega}} \chi_{ik}(\omega) \mu_{kj}, \quad (2)$$

where $\chi_{ij}(\omega) = i \langle \langle \sigma_i; \sigma_j \rangle \rangle / \hbar$ is the spin-spin response function studied in Refs. 26 and 27.

In the limit of vanishing temperature the spin susceptibility takes the form

$$\chi_{ij}(\omega) = \int' \frac{d^2k}{(2\pi)^2} \left(\frac{M_{ij}(\mathbf{k})}{\Delta(\mathbf{k}) - \hbar \tilde{\omega}} + \frac{M_{ji}(\mathbf{k})}{\Delta(\mathbf{k}) + \hbar \tilde{\omega}} \right), \quad (3)$$

where $M_{ij}(\mathbf{k}) = \langle -|\sigma_i| + \rangle \langle +|\sigma_j| - \rangle$. The prime on the integral sign means that integration is restricted to the \mathbf{k} region lying between the Fermi contours $k_F^+(\theta) < k < k_F^-(\theta)$, for which $\varepsilon_-(\mathbf{k}) < \varepsilon_F < \varepsilon_+(\mathbf{k})$. The matrix elements are given by the expression

$$\Omega_\parallel^2 \Omega^2 M_{\mu\mu'} = -\Omega_\parallel^2 [\Omega_{\parallel\mu} \Omega_{\parallel\mu'} - \delta_{\mu\mu'} \Omega^2] + \Omega_\parallel^4 \delta_{\mu\mu'} \delta_{\mu z}$$

$$- \Omega_z \Omega_\parallel^2 (\Omega_{\parallel\mu} \hat{\mathbf{e}}_{\mu'} + \Omega_{\parallel\mu'} \hat{\mathbf{e}}_\mu) \cdot \hat{\mathbf{z}} - i \Omega \Omega_\parallel^2 \Omega_\parallel \cdot (\hat{\mathbf{e}}_\mu$$

$$\times \hat{\mathbf{e}}_{\mu'}) + i \Omega_z \Omega \Omega_\parallel \cdot [\hat{\mathbf{z}} \times (\Omega_{\parallel\mu} \hat{\mathbf{e}}_{\mu'} - \Omega_{\parallel\mu'} \hat{\mathbf{e}}_\mu)],$$

where $\mathbf{\Omega}_\parallel = (\Omega_x, \Omega_y, 0)$ and $\hat{\mathbf{e}}_\mu$ is the unit vector in the direction $\mu = x, y, \text{ or } z$, ($\hat{\mathbf{z}} = \hat{\mathbf{e}}_z$). We note that the matrix elements depend only on the polar angle θ and that $M_{\mu'\mu} = M_{\mu\mu}^*$. Using this, the susceptibility tensor Eq. (3) can be written in the form $\chi_{ij} = \chi'_{ij} + i\chi''_{ij}$ with

$$\chi'_{ij}(\omega) = \chi_{ij}(0) + \frac{\hbar\omega}{16\pi^2} \int_0^{2\pi} d\theta \frac{M'_{ij}(\theta)}{g^2(\theta)} \times \log \left| \frac{[\omega + \omega_+(\theta)][\omega - \omega_-(\theta)]}{[\omega + \omega_-(\theta)][\omega - \omega_+(\theta)]} \right| + I'_{ij}(\omega),$$

$$\chi''_{ij}(\omega) = \frac{\hbar\omega}{16\pi} \int d\theta \frac{M''_{ij}(\theta)}{g^2(\theta)} \Theta[\omega - \omega_+(\theta)] \Theta[\omega - \omega_-(\theta)] + I''_{ij}(\omega),$$

where $\chi_{ij}(0) = (\nu_0/2\pi) \int_0^{2\pi} M'_{ij}(\theta) d\theta$ is the static value, $\nu_0 = m/\pi\hbar^2$, and

$$I'_{ij}(\omega) = -\frac{\hbar\omega}{16\pi} \int d\theta \frac{M''_{ij}(\theta)}{g^2(\theta)} \Theta[\omega - \omega_+(\theta)] \Theta[\omega - \omega_-(\theta)],$$

$$I''_{ij}(\omega) = \frac{\hbar\omega}{16\pi^2} \int_0^{2\pi} d\theta \frac{M''_{ij}(\theta)}{g^2(\theta)} \log \left| \frac{\omega^2 - \omega_-^2(\theta)}{\omega^2 - \omega_+^2(\theta)} \right|.$$

The functions $\omega_{\pm}(\theta)$ are given by $\hbar\omega_{\pm}(\theta) = \Delta[k_F^{\pm}(\theta), \theta]$

$$\hbar\omega_+(\theta) = \varepsilon_F - \varepsilon_-[k_F^+(\theta), \theta],$$

$$\hbar\omega_-(\theta) = \varepsilon_+[k_F^-(\theta), \theta] - \varepsilon_F,$$

and correspond to the minimum (+) and maximum (−) energies required to make an allowed vertical transition between spin-split subbands for a given direction θ in momentum space. Numerical evaluation shows that $I'_{ij} = I''_{ij} = 0$ for each grown direction $[hkl]$. In these expressions the product of unit step functions $\Theta(x)$ arises from integrals involving the delta function $\delta[\varepsilon_+(\mathbf{k}) - \varepsilon_-(\mathbf{k}) - \hbar\omega]$, describing a photon-absorption process. Thus, there will be a contribution whenever the photon energy $\hbar\omega$ and the spin-splitting energy $\Delta(k, \theta) = 2kg_{[hkl]}(\theta)$ match for states with k lying between the Fermi contours $k_F^{\lambda}(\theta)$. Hence, for a given frequency, the integral giving $\chi''_{ij}(\omega)$ is restricted to angular regions for which $\omega_+(\theta) \leq \omega \leq \omega_-(\theta)$ [see Figs. 1(b) and 2(b)].

For a QW grown in the [001] direction, we found that

$$\begin{pmatrix} S_x(\omega) \\ S_y(\omega) \end{pmatrix} = \frac{\hbar}{2} \begin{pmatrix} \gamma_{xx} & \gamma_{xy} \\ -\gamma_{xy} & -\gamma_{xx} \end{pmatrix} \begin{pmatrix} E_x(\omega) \\ E_y(\omega) \end{pmatrix} \quad (4)$$

or in vectorial form

$$\mathbf{S}(\omega) = (\hbar/2)[\gamma_{xx}(\omega)(E_x\hat{x} - E_y\hat{y}) + \gamma_{xy}(\omega)\mathbf{E} \times \hat{z}]$$

with

$$\begin{aligned} \gamma_{ij}(\omega) &= \frac{e}{i\hbar\omega} [\chi_{ix}(\omega)(\alpha\delta_{jy} - \beta_{[001]}\delta_{jx}) \\ &+ \chi_{iy}(\omega)(\beta_{[001]}\delta_{jy} - \alpha\delta_{jx})], \end{aligned} \quad (5)$$

where we have used Eq. (2) and the results $\chi_{xx}(\omega) = \chi_{yy}(\omega)$, $\chi_{xy}(\omega) = \chi_{yx}(\omega)$, and $\chi_{zj}(\omega) = 0$.

For a [110]-grown QW we obtain

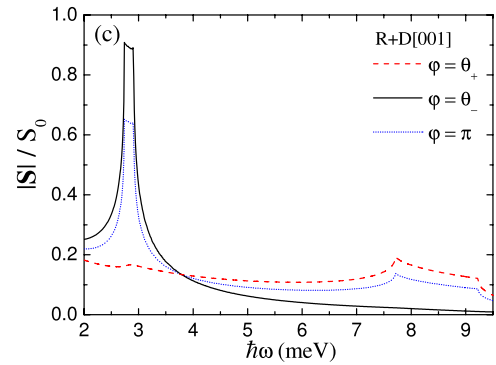
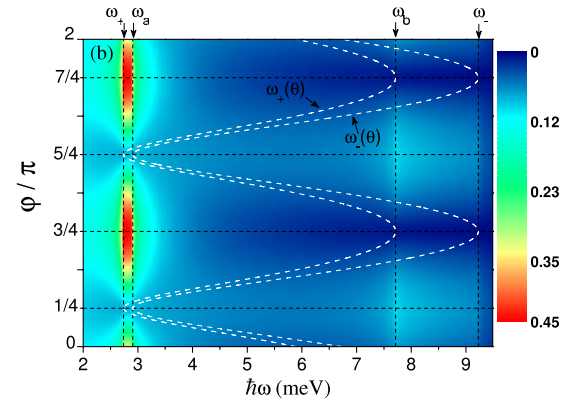
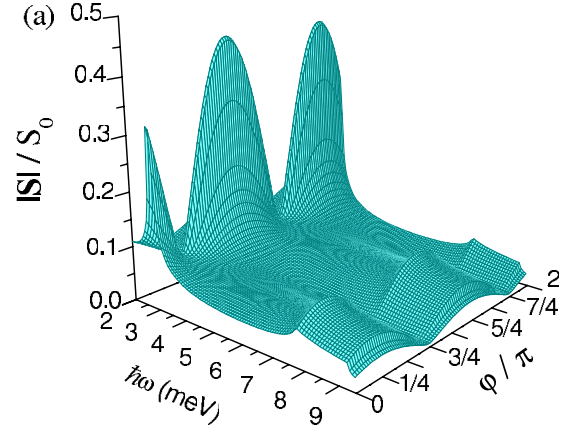


FIG. 1. (Color online) Spin-polarization density S of a [001]-grown quantum well with Rashba and linear Dresselhaus SO couplings. (a) The magnitude S vs photon energy $\hbar\omega$ and the electric field angle φ . (b) Contour map of $S(\omega, \varphi)$. The functions $\hbar\omega_{\pm}(\theta) = 2k_F^{\pm}(\theta)g_{[001]}(\theta)$ delimit the angular region in \mathbf{k} space available for optical transitions. The special frequencies $\omega_{\pm}(\theta_{\pm})$ and $\omega_{\mp}(\theta_{\pm})$ are indicated (see text). (c) $S(\omega)$ for several directions of the applied in-plane electric field. Here $\theta_+ = \pi/4$ and $\theta_- = 3\pi/4$ are directions of symmetry in momentum space. The parameter used are $m = 0.055m_0$, $n = 5 \times 10^{11} \text{ cm}^{-2}$, $\alpha = 160 \text{ meV \AA}$, and $\beta_{[001]} = 0.5\alpha$. The polarization is normalized to the value at the spin splitting energy $\Delta_D = 2\beta k_F$, $S_0 = (\hbar/2)|\gamma_{yy}(\omega = \Delta_D/\hbar)|E$.

$$\begin{pmatrix} S_x(\omega) \\ S_y(\omega) \\ S_z(\omega) \end{pmatrix} = \frac{\hbar}{2} \begin{pmatrix} 0 & \gamma_{xy} & 0 \\ \gamma_{yx} & 0 & 0 \\ \gamma_{zx} & 0 & 0 \end{pmatrix} \begin{pmatrix} E_x(\omega) \\ E_y(\omega) \\ 0 \end{pmatrix}, \quad (6)$$

that is,

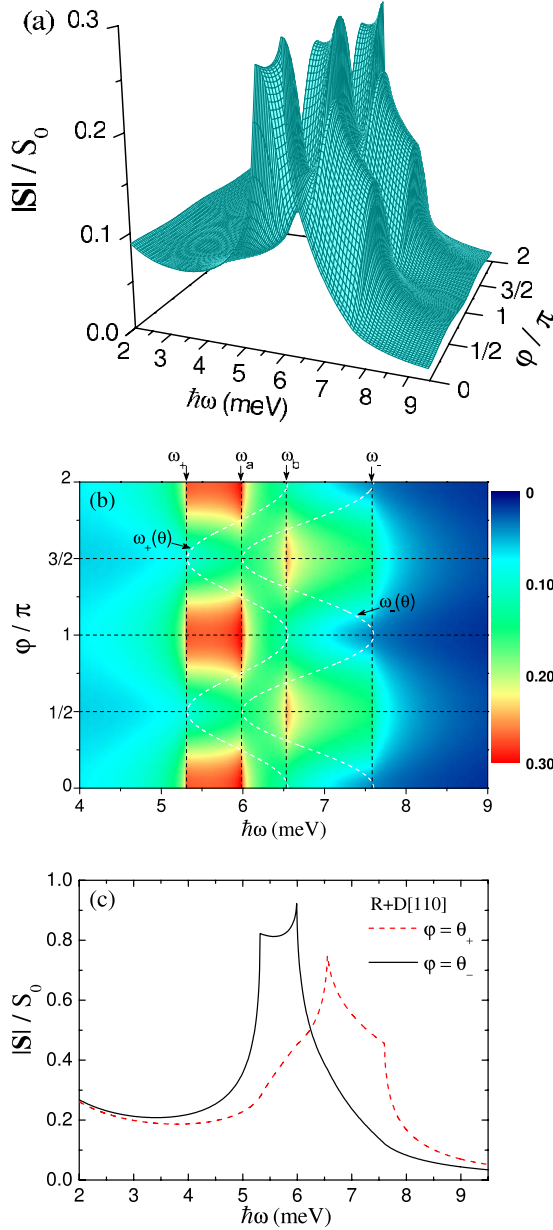


FIG. 2. (Color online) Spin polarization density $S(\omega, \varphi)$ as in Fig. 1 but for a [110] quantum well. Here $\theta_+ = \pi/2$, $\theta_- = 0$, and $\beta_{[110]} = 0.75\alpha$.

$$\mathbf{S}(\omega) = (\hbar/2)[\gamma_{xy}(\omega)E_y\hat{\mathbf{x}} + \gamma_{yx}(\omega)E_x\hat{\mathbf{y}} + \gamma_{zx}(\omega)E_x\hat{\mathbf{z}}],$$

where $\gamma_{zx}(\omega) = -(\beta_{[110]}/\alpha)\gamma_{yx}(\omega)$. In this case $\chi_{xy} = \chi_{yx} = \chi_{xz} = \chi_{zx} = 0$, $\chi_{yz} = \chi_{zy}$, and

$$\gamma_{ij}(\omega) = \frac{e}{i\hbar\omega}[\alpha\chi_{ix}(\omega)\delta_{jy} - \alpha\chi_{iy}(\omega)\delta_{jx} + \beta_{[110]}\chi_{iz}(\omega)\delta_{jx}]. \quad (7)$$

For the [111] direction of growth, $\gamma_{ij}(\omega) = \gamma_{xy}(\omega)\epsilon_{ijz}$ with $\gamma_{xy}(\omega) = e\tilde{\alpha}\chi_{xx}(\omega)/i\hbar\omega$, which implies

$$\mathbf{S}(\omega) = (\hbar/2)\gamma_{xy}(\omega)\mathbf{E} \times \hat{\mathbf{z}}$$

or

$$\begin{pmatrix} S_x(\omega) \\ S_y(\omega) \end{pmatrix} = \frac{\hbar}{2} \begin{pmatrix} 0 & \gamma_{xy} \\ -\gamma_{xy} & 0 \end{pmatrix} \begin{pmatrix} E_x(\omega) \\ E_y(\omega) \end{pmatrix}, \quad (8)$$

here we used the results $\chi_{xx} = \chi_{yy}$ and $\chi_{xy} = \chi_{yx} = 0$.

IV. RESULTS

It can be seen from these expressions that in the case of anisotropic spin splitting the magnitude $S = |\mathbf{S}|$ of the spin polarization depends not only on the excitation frequency but also on the direction of the applied electric field $\mathbf{E} = E(\cos\varphi\hat{\mathbf{x}} + \sin\varphi\hat{\mathbf{y}})$. While for the R+D[111] case Eq. (8) implies $S(\omega) = (\hbar/2)|\gamma_{xy}(\omega)|E$, which is independent of the electric field angle φ , for R+D[001] and R+D[110] Eqs. (4) and (6) yield

$$S^2(\omega, \varphi) = \left(\frac{\hbar}{2}E\right)^2 [|\gamma_{xx}|^2 + |\gamma_{yy}|^2 + 2\text{Re}(\gamma_{xx}\gamma_{yy}^*)\sin 2\varphi] \quad (9)$$

and

$$S^2(\omega, \varphi) = \left(\frac{\hbar}{2}E\right)^2 \frac{1}{2} [|\gamma_{yx}|^2 + |\gamma_{xz}|^2 + |\gamma_{xy}|^2 + (|\gamma_{yx}|^2 + |\gamma_{xz}|^2 - |\gamma_{xy}|^2)\cos 2\varphi], \quad (10)$$

respectively. This anisotropic response is shown in Figs. 1 and 2 for the [001]- and [110]-grown directions, as calculated using Eqs. (5) and (7) and from numerical evaluation of expression (3). For a given value of φ , as a function of frequency, the magnitude $S(\omega, \varphi)$ can display structure at some well-identified frequencies determined by the anisotropic \mathbf{k} space available for optical transitions.²⁷ According to the nonisotropic spin splitting caused by the simultaneous presence of the Rashba and Dresselhaus couplings, the minimum (maximum) photon energy $\hbar\omega_+$ ($\hbar\omega_-$) required to induce vertical transitions between the initial $\lambda = -$ and final $\lambda = +$ spin-split subbands corresponds to an excitation at a wave vector lying on the Fermi line k_F^+ (k_F^-) along the direction $\theta = \theta_+$ (θ_-) where the spin splitting takes its minimum (maximum) value. These directions are $\theta_+ = \pi/4$ and $\theta_- = 3\pi/4$ for R+D[001] and $\theta_+ = \pi/2$ and $\theta_- = 0$ for R+D[110]. In Figs. 1(b) and 2(b), these particular energies $\hbar\omega_{\pm} = \hbar\omega_{\pm}(\theta_{\pm})$ are indicated along with the functions $\hbar\omega_{\pm}(\theta)$ which reveal the angular region between Fermi contours available for direct transitions at energy $\hbar\omega$.

The other two vertical lines at the frequencies labeled as ω_a and ω_b are given by $\hbar\omega_-(\theta_+)$ and $\hbar\omega_+(\theta_-)$, respectively. At these energies the joint density of states (JDOS) shows singularities due to the presence of critical points of the energy-difference function $\Delta(k, \theta)$.²⁵ For a given frequency the JDOS is given by a line integral of $(\hbar v_{\mathbf{k}})^{-1} = |\nabla_{\mathbf{k}}\Delta(\mathbf{k})|^{-1}$ carried out over those portions of the curve $C_r(\omega)$ of constant interband energy, $\Delta(k, \theta) - \hbar\omega = 0$, lying within the regions enclosed by the Fermi lines $k_F^{\pm}(\theta)$. The peaks in the JDOS appear due to electronic excitations involving states with allowed wave vectors on $C_r(\omega)$ such that $v_{\mathbf{k}}$ takes extreme values. The resonance curve $C_r(\omega)$ is given by the quadratic form $(\hbar\omega/2)^2 = \mu_{ij}\mu_{il}k_jk_l$ which for the anisotropic cases of

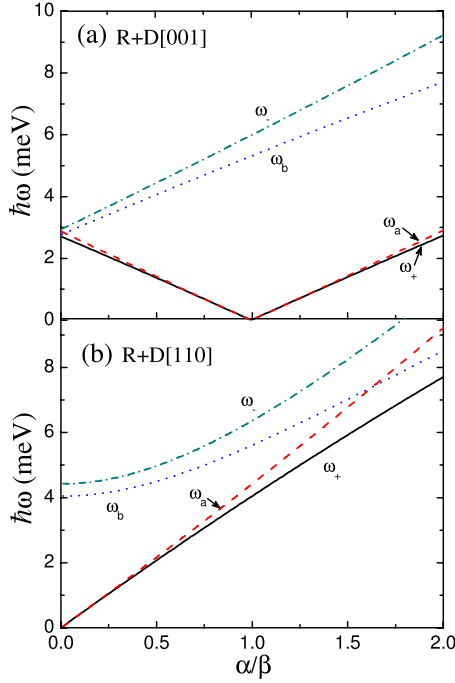


FIG. 3. (Color online) The absorption edges $\omega_{\pm} = \omega_{\pm}(\theta_{\pm})$ and critical frequencies $\omega_a = \omega_-(\theta_+)$ and $\omega_b = \omega_+(\theta_-)$ as a function of the Rashba parameter $\alpha/\beta_{[hkl]}$, for (a) [001] quantum well with $\beta_{[001]} = 80$ meV Å and (b) [110] quantum well with $\beta_{[110]} = 120$ meV Å. Other parameters are the same as in Fig. 1.

Figs. 1 and 2 is a rotated ellipse with semiaxis of lengths (major) $k_a(\omega) = \hbar\omega/2g_{[hkl]}(\theta_+)$ and (minor) $k_b(\omega) = \hbar\omega/2g_{[hkl]}(\theta_-)$ oriented along θ_+ and θ_- symmetry directions, respectively. The photon energy $\hbar\omega_a$ ($\hbar\omega_b$) corresponds to the resonance condition for which $k_a(\omega) = k_F^-(\theta_+)$ [$k_b(\omega) = k_F^+(\theta_-)$]. Figure 3 shows the frequencies $\omega_{\pm}(\theta_{\pm})$ and $\omega_{\pm}(\theta_{\pm})$ as a function of the Rashba SO-coupling strengths α , for a given value of $\beta_{[hkl]}$. When $\alpha = \beta_{[001]}$ in a [001] QW or $\alpha = 0$ in a [110] QW, the spin splitting vanishes along $\theta = \theta_+$ direction, $g_{[hkl]}(\theta_+) = 0$, and then $\omega_+ = \omega_a = 0$.

As for the dependence on the direction of the in-plane electric field vector, we observe that as a function of φ , $S(\omega, \varphi)$ follows the same functional angular dependence as that of the splitting function $g_{[hkl]}$. This anisotropic character modifies the size of the response appreciably. For instance, in the case of a sample with R+D[001] SOI, it is found that the peak in the vicinity of ω_a at $\varphi = \theta_-$ can be considerably suppressed if the electric field orientation is changed to be aligned along $\varphi = \theta_+$ direction. Moreover, as frequency varies this behavior notably changes [Fig. 1(c)]. At $\varphi = \theta_{\pm}$, expression (9) reduces to $S(\omega, \varphi = \theta_{\pm}) \propto (1/\omega) |\alpha \mp \beta_{[001]}| |\chi_{xx}(\omega) \mp \chi_{xy}(\omega)|$ and it turns out that around ω_a , $\chi_{xx}(\omega) \approx \chi_{xy}(\omega)$ while at higher frequencies close to ω_b , $\chi_{xx}(\omega) \approx -\chi_{xy}(\omega)$. This introduces a strong cancellation for $\varphi = \theta_-$ when $\omega \approx \omega_b$, as is observed in Fig. 1(c). Similar behavior is observed in the R+D[110] SOI case, within the corresponding narrower range of frequencies [Fig. 2(c)]. The φ dependence of S of the form $g_{[hkl]}(\varphi)$ [Eqs. (9) and (10)] illustrates the role of R+D SOI behind the physical origin of such anisotropic behavior.

The frequency dependence of spin-polarization density $S(\omega, \varphi)$ for a continuous variation in the ratio $\alpha/\beta_{[hkl]}$, for a

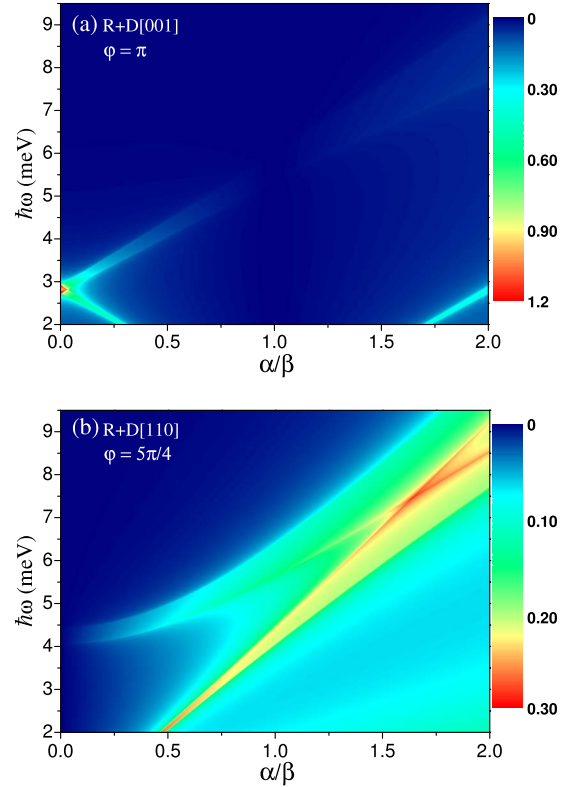


FIG. 4. (Color online) Contour map of the spin polarization S of [001] and [110] quantum wells vs photon energy and the Rashba parameter $\alpha/\beta_{[hkl]}$, for a fixed value of the electric field angle φ . Sample parameters are as those used in Fig. 3.

fixed value of the electric field angle φ , is showed in Fig. 4. The main features of the spectrum exhibit the same variation with parameter α as that followed for the absorption frequency edges ω_{\pm} and the critical frequencies ω_a and ω_b (Fig. 3). In Fig. 4(b), the highest magnitude takes place at the point where $\omega_a(\alpha)$ and $\omega_b(\alpha)$ cross each other [Fig. 3(b)]. This is a consequence of the fact that at photon energies $\hbar\omega$ coinciding with the particular value $\hbar\omega^* = \hbar\omega_a = \hbar\omega_b$, the semiaxes $k_a(\omega^*)$ and $k_b(\omega^*)$ take the values $k_F^-(\theta_+)$, $k_F^+(\theta_-)$, respectively. Thus, the whole ellipse $C_r(\omega^*)$ lies between the Fermi contours and gives a larger contribution to the JDOS. We have also verified that the spin-density polarization vanishes for all frequencies when $\alpha = 0$ in the R+D[110] case or at the point $\alpha = \beta_{[001]}$ in the case of R+D[001] SOI, as was predicted in Ref. 14. This remarkably property, taking place at that particular values of the SO strength parameters, has been explained by the existence of a fixed (momentum-independent) precession axis leading to the suppression of the Dyakonov-Perel spin-relaxation mechanism.^{14,15,18}

It has been established previously that there is a connection between the spin-density response and the charge- or spin-current response.¹⁴ The SO contribution to the charge current conductivity $\sigma_{ij}^{SO}(\omega) = \langle\langle ev_i; ev_j \rangle\rangle / \hbar\tilde{\omega}$, due to the interspin-split (vertical) transitions,²⁵ can be related to the spin-polarizability tensor γ_{ij} through $\sigma_{ij}^{SO}(\omega) = e\mu_{ki}\gamma_{kj}(\omega)/\hbar$, and to the spin conductivity through $\sigma_{ij}^{SO}(\omega) = (4iem/\hbar^4\tilde{\omega})\epsilon_{kpq}\mu_{pi}\mu_{ql}\Sigma_{ij}^k(\omega)$. The function Σ_{ij}^k gives the

spin current \mathcal{J}_i^k flowing in the i direction with the spin polarized in the k direction as a response to the j component of an electric field, and it is obtained from the spin-current-charge-current Kubo formula $\Sigma_{ij}^k(\omega) = \langle\langle \hat{\mathcal{J}}_i^k; ev_j \rangle\rangle / \hbar \tilde{\omega}$. A relation between the spin polarizability and the spin-current response then reads as $\gamma_{ij}(\omega) = (4im/\hbar^3 \tilde{\omega}) \epsilon_{iqp} \mu_{ql} \Sigma_{lj}^p(\omega)$. These relations imply that all the response functions will exhibit similar spectral features in their frequency dependence. It can also be expected that the induced quantities will display the same anisotropic behavior with respect to the direction of the applied electric field.

Our results are important to the spintronic four-terminal device proposed in Ref. 19. This is based on the static spin-density response and was devised to study the variation in the spin accumulation in a 2DEG with R+D[001] SOI when the electric field orientation is changed. Our calculations show that such anisotropic property can be further modulated by adjusting the frequency of the exciting field. This additional controllability could be useful in experimental studies of this type of magnetoelectric effect.

V. SUMMARY

In summary, the finite-frequency spin-polarizability tensor of a 2DEG with anisotropic SOI shows strong variations and spectral features significantly different from that of an isotropic SOI case. The spectral features in the spin response of quantum wells grown in the [001] and [110] crystallographic directions are explained in terms of the anisotropic momentum space available for direct transitions, given the particular angular dependence of the spin splitting introduced by the interplay between the Rashba and Dresselhaus SO mechanisms in each case. Remarkably, the magnitude of the induced spin polarization becomes dependent on the direction of the applied electric field. This anisotropy combined with such frequency dependence and the tunability of the Rashba interaction, suggests new possibilities of manipulation of the spin-density response which could find spintronic applications.

ACKNOWLEDGMENT

We acknowledge the support from DGAPA-UNAM under Grant No. IN114210.

-
- ¹V. M. Edelstein, *Solid State Commun.* **73**, 233 (1990); A. G. Aronov, Yu. B. Lyanda-Geller, and G. E. Pikus, *Sov. Phys. JETP* **73**, 537 (1991).
- ²E. I. Rashba, *Physica E* **20**, 189 (2004).
- ³N. P. Stern, S. Ghosh, G. Xiang, M. Zhu, N. Samarth, and D. D. Awschalom, *Phys. Rev. Lett.* **97**, 126603 (2006).
- ⁴D. Culcer and R. Winkler, *Phys. Rev. Lett.* **99**, 226601 (2007).
- ⁵I. Žutić, J. Fabian, and S. Das Sarma, *Rev. Mod. Phys.* **76**, 323 (2004).
- ⁶E. G. Mishchenko, A. V. Shytov, and B. I. Halperin, *Phys. Rev. Lett.* **93**, 226602 (2004).
- ⁷H. C. Koo, J. H. Kwon, J. Eom, J. Chang, S. H. Han, and M. Johnson, *Science* **325**, 1515 (2009).
- ⁸Y. K. Kato, R. C. Myers, A. C. Gossard, and D. D. Awschalom, *Phys. Rev. Lett.* **93**, 176601 (2004).
- ⁹A. Yu. Silov, P. A. Blajnov, J. H. Wolter, R. Hey, K. H. Ploog, and N. S. Averkiev, *Appl. Phys. Lett.* **85**, 5929 (2004).
- ¹⁰V. Sih, R. C. Myers, Y. K. Kato, W. H. Lau, A. C. Gossard, and D. D. Awschalom, *Nat. Phys.* **1**, 31 (2005).
- ¹¹S. D. Ganichev, S. N. Danilov, P. Schneider, V. V. Bel'kov, L. E. Golub, W. Wegscheider, D. Weiss, and W. Prettl, *J. Magn. Magn. Mater.* **300**, 127 (2006).
- ¹²C. L. Yang, H. T. He, L. Ding, L. J. Cui, Y. P. Zeng, J. N. Wang, and W. K. Ge, *Phys. Rev. Lett.* **96**, 186605 (2006).
- ¹³J. Schliemann, J. C. Egues, and D. Loss, *Phys. Rev. Lett.* **90**, 146801 (2003).
- ¹⁴O. E. Raichev, *Phys. Rev. B* **75**, 205340 (2007).
- ¹⁵V. V. Bryksin and P. Kleinert, *Int. J. Mod. Phys. B* **20**, 4937 (2006).
- ¹⁶B. A. Bernevig, J. Orenstein, and S.-C. Zhang, *Phys. Rev. Lett.* **97**, 236601 (2006); P. Kleinert and V. V. Bryksin, *Phys. Rev. B* **76**, 205326 (2007).
- ¹⁷J. D. Koralek, C. P. Weber, J. Orenstein, B. A. Bernevig, S.-C. Zhang, S. Mack, and D. D. Awschalom, *Nature (London)* **458**, 610 (2009).
- ¹⁸M. Duckheim, D. Loss, M. Scheid, K. Richter, I. Adagideli, and P. Jacquod, *Phys. Rev. B* **81**, 085303 (2010).
- ¹⁹M. Trushin and J. Schliemann, *Phys. Rev. B* **75**, 155323 (2007).
- ²⁰S. M. Badalyan, A. Matos-Abiague, G. Vignale, and J. Fabian, *Phys. Rev. B* **79**, 205305 (2009).
- ²¹A. V. Chaplik, M. V. Entin, and L. I. Magarill, *Physica E* **13**, 744 (2002).
- ²²E. I. Rashba, *Phys. Rev. B* **70**, 161201 (2004); *J. Supercond.* **18**, 137 (2005).
- ²³A. Shekhter, M. Khodas, and A. M. Finkel'stein, *Phys. Rev. B* **71**, 165329 (2005).
- ²⁴M. Duckheim, D. L. Maslov, and D. Loss, *Phys. Rev. B* **80**, 235327 (2009).
- ²⁵J. A. Maytorena, C. López-Bastidas, and F. Mireles, *Phys. Rev. B* **74**, 235313 (2006).
- ²⁶S. I. Erlingsson, J. Schliemann, and D. Loss, *Phys. Rev. B* **71**, 035319 (2005).
- ²⁷C. López-Bastidas, J. A. Maytorena, and F. Mireles, *Phys. Status Solidi C* **4**, 4229 (2007).
- ²⁸E. Ya. Sherman, A. Najmaie, and J. E. Sipe, *Appl. Phys. Lett.* **86**, 122103 (2005).
- ²⁹M. Pletyukhov and A. Shnirman, *Phys. Rev. B* **79**, 033303 (2009).
- ³⁰A. Wong, J. A. Maytorena, C. López-Bastidas, and F. Mireles, *Phys. Rev. B* **77**, 035304 (2008).
- ³¹X. Cartoixà, D. Z.-Y. Ting, and Y.-C. Chang, *Phys. Rev. B* **71**, 045313 (2005).